Electronic Supplementary Material (ESI) for Environmental Science: Atmospheres.

Supplement for:

Observed in-plume gaseous elemental mercury depletion suggests significant mercury scavenging by volcanic aerosols

Alkuin M. Koenig et al.

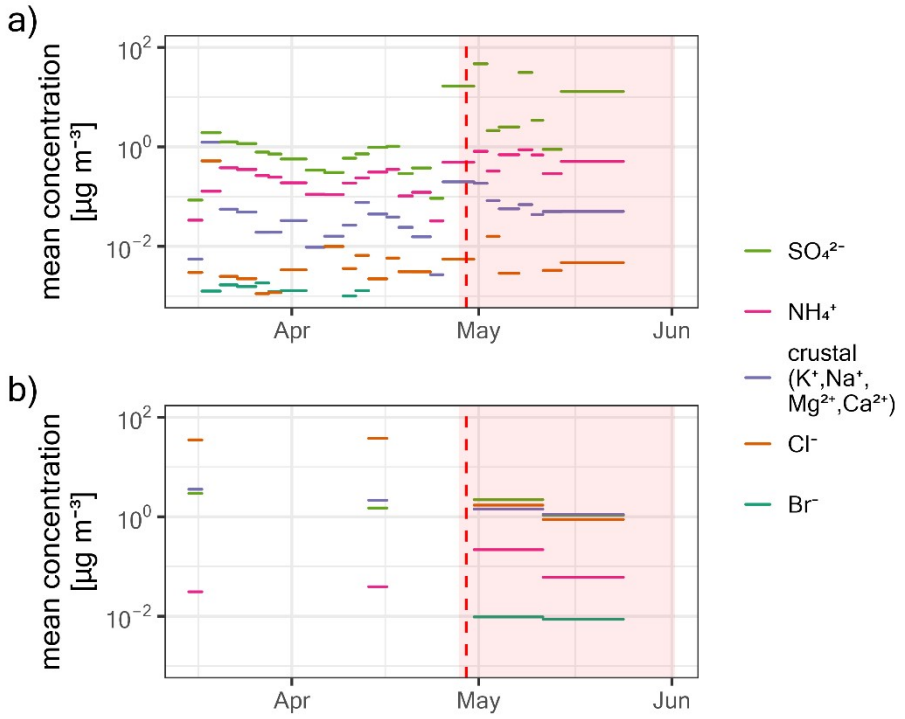

Figure S1. *Comparison of inorganic ion concentrations in* ***(a)*** *submicron and* ***(b)*** *supermicron aerosols. All concentrations are given at STP. The dashed vertical line corresponds to the day of observed GEM depletion (April 29th). Note the data gaps for supermicron aerosols observations.*

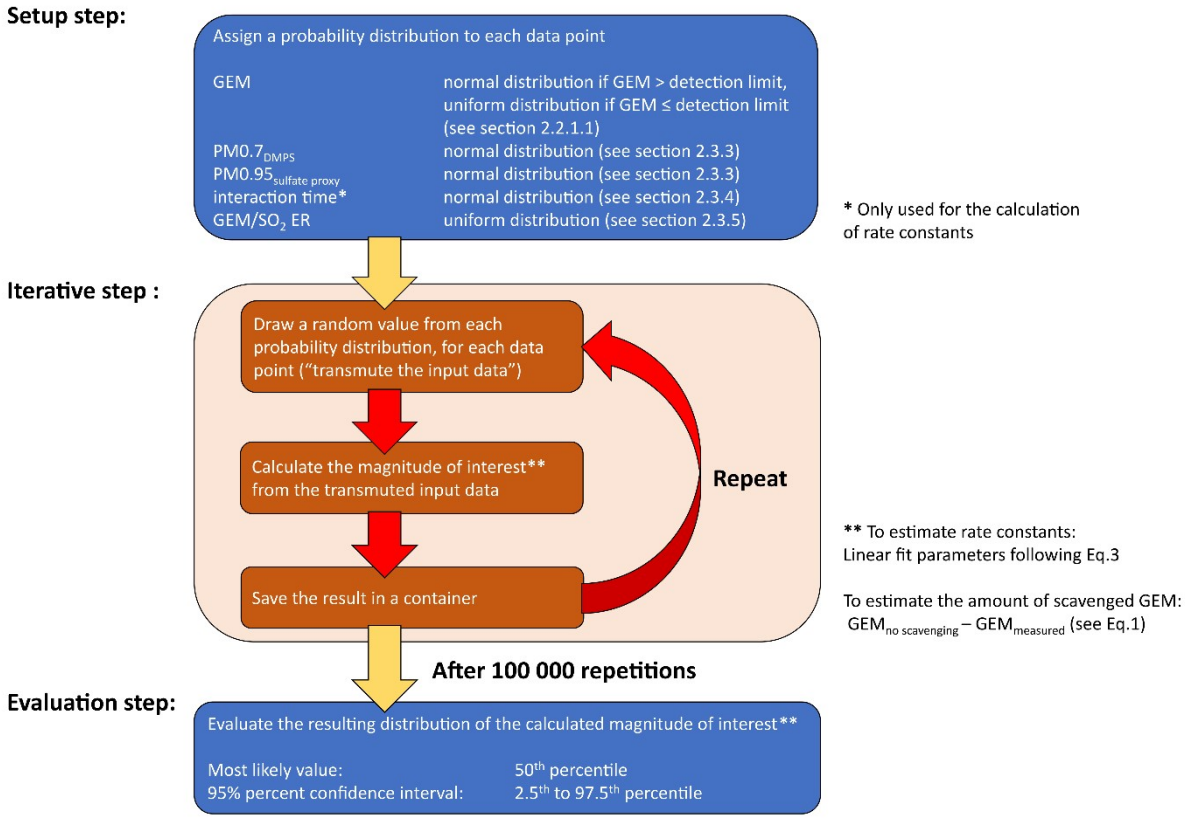

Figure S2. *Schematized representation of the procedure followed to perform the Monte Carlo simulations.*

Table S1. *Summary of literature Hg/SO_2 mass ratios obtained from measurements of volcanic plume gases from hotspot/rift and arc volcanoes since the year 2000.*

Volcano	Location	Tectonic setting	Hg/SO_2	Reference
Ambrym	Vanuatu	Arc	6.4×10^{-6}	Bagnato et al., 2011
Ambrym	Vanuatu	Arc	9.0×10^{-6}	Allard et al., 2016
Yasur	Vanuatu	Arc	1.7×10^{-5}	Bagnato et al., 2011
Miyake-jima	Japan	Arc	2.4×10^{-6}	Friedli et al., 2004
Miyake-jima	Japan	Arc	9.0×10^{-6}	Bagnato et al., 2011
Turrialba	Costa Rica	Arc	6.0×10^{-6}	Bagnato et al., 2014
Gorely	Alaska	Arc	3.3×10^{-6}	Bagnato et al., 2011
La Soufrière	Saint Vincent	Arc	1.2×10^{-5}	Bagnato et al., 2011
Popocatépetl	Mexico	Arc	2.0×10^{-4}	Schiavo et al., 2020
Stromboli	Italy	Arc	4.7×10^{-6}	Bagnato et al., 2011
Etna, Stromboli, Vulcano	Italy	Composite, Arc	1.5×10^{-7}	Ferrara et al., 2000
Etna	Italy	Composite	8.8×10^{-6}	Bagnato et al., 2007
Etna	Italy	Composite	5.2×10^{-6}	Bagnato et al., 2014
Nyiragongo	DRC	Hotspot/rift	5.5×10^{-6}	Bagnato et al., 2011
Kīlauea	Hawai‘i	Hotspot/rift	1.0×10^{-6}	Mather et al., 2012
Erebus	Antarctica	Hotspot/rift	2.0×10^{-5}	Wardell et al., 2008
Fagradalsfjall	Iceland	Hotspot/rift	6.7×10^{-7}	Edwards et al., 2021

Table S2. *Overview statistics of reported Hg/SO_2 emission ratios since the year 2000 (see Table S1).*

Statistic	Hg/SO_2 emission ratio (mass ratio)
0^{th} percentile (minimum)	1.5×10^{-7}
10^{th} percentile	8.4×10^{-7}
50^{th} percentile (median)	5.4×10^{-6}
90^{th} percentile	1.6×10^{-5}
100^{th} percentile (maximum)	2.0×10^{-4}

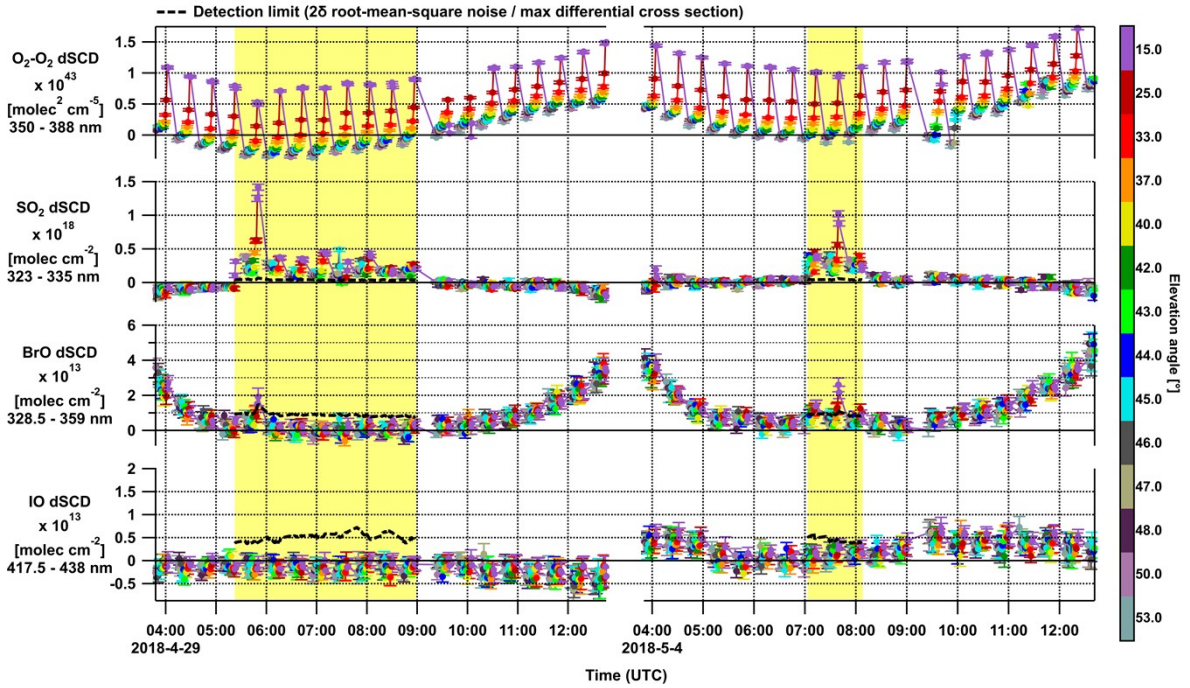

Figure S3. *O_2-O_2, SO_2, BrO, and IO dSCDs measured by the CU MAX-DOAS instrument on April 29 and May 4, 2018. The marker colors indicate the individual elevation angles (above the horizon). The yellow shading indicates periods of elevated SO_2 dSCDs due to the volcanic plume. The black dashed lines indicate the detection limits during the volcanic plume periods. The diurnal curvature of the BrO dSCDs is due to stratospheric BrO.*

Table S3. *Estimation of GEM lifetime against oxidation by Br in daytime plumes from Piton de la Fournaise. Rate constants from (Shah et al., 2021)*

Reactions			
Reactants	**Products**	**rate constant**	**comment**
Br + GEM	Br.GEM	k1	
Br.GEM	Br + GEM	k-1	thermal decomposition; k0/Keq; Keq = 9.14 × 10−24 exp(7801/T)
Br.GEM + O3	Br.GEM.O + O2	k2	
Input magnitudes			
Magnitude	**value**	**unit**	
O3	40	ppbv	
Br	1.2	pptv	Assuming 1 ppmv SO2, BrO/SO2 = 1.2e-5 (measured), and Br/BrO = 0.1
Temperature	288	K	
Pressure	0.8	atm	
Transport time	3	hrs	
Calculated magnitudes			
Magnitude	**value**	**unit**	
M	2.03E+19	molec cm^{-3}	
k1	3.16E-13	cm3 $molec^{-1}$ s^{-1}	
k1*[Br]	7.71E-06	s^{-1}	
tau_GEM	3.60E+01	hrs	
k-1	5.96E-02	s^{-1}	
tau_decomp	1.68E+01	s	
k2	3.00E-11		
k2*[O3]	2.44E+01	s^{-1}	
tau_HgII	4.10E-02	s	
Output:			
GEM lifetime in plume:	35.9	hrs	
GEM oxidation after 5 hours (light conditions)	~13.0	%	

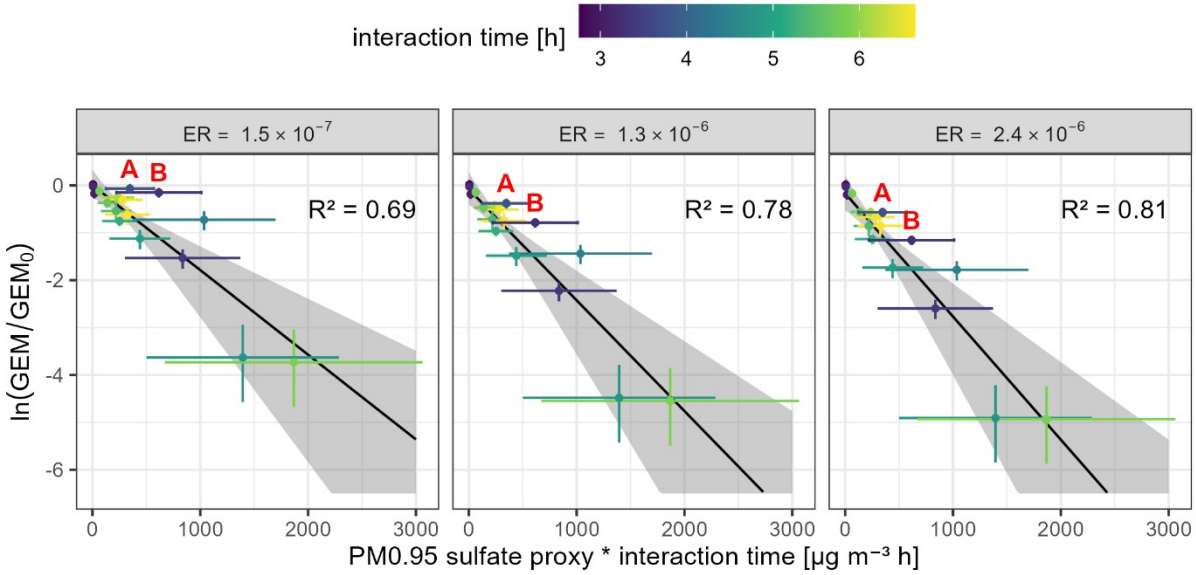

Figure S4. *Observed GEM depletion in function of $PM0.95_{sulfate\ proxy}$ and interaction time, and for three different possible GEM/SO_2 emission ratios from Piton de la Fournaise (corresponding to the minimum, median, and maximum of the uniform probability distribution assigned to the GEM/SO_2 emission ratio. The error bars indicate 95% confidence intervals and the shaded area shows the 95% confidence interval of the fit (Monte Carlo simulation). The color scale shows the estimated mean interaction time between volcanic particles and GEM before the plume's arrival at Maïdo. The figure and the linear regressions are based on all observations between 3:55 and 10:10 local time. Data points marked with "A" and "B" correspond to the most notable outliers, sampled between 5:10 - 5:25 and 5:40 - 5:55 local time, respectively. Fit parameters are shown in Figure 5 of the main text.*

References:

Allard, P., Aiuppa, A., Bani, P., Métrich, N., Bertagnini, A., Gauthier, P.-J., Shinohara, H., Sawyer, G., Parello, F., Bagnato, E., Pelletier, B., and Garaebiti, E.: Prodigious emission rates and magma degassing budget of major, trace and radioactive volatile species from Ambrym basaltic volcano, Vanuatu island Arc, Journal of Volcanology and Geothermal Research, 322, 119–143, https://doi.org/10.1016/j.jvolgeores.2015.10.004, 2016.

Bagnato, E., Aiuppa, A., Parello, F., Calabrese, S., D'Alessandro, W., Mather, T. A., McGonigle, A. J. S., Pyle, D. M., and Wängberg, I.: Degassing of gaseous (elemental and reactive) and particulate mercury from Mount Etna volcano (Southern Italy), Atmospheric Environment, 41, 7377–7388, https://doi.org/10.1016/j.atmosenv.2007.05.060, 2007.

Bagnato, E., Aiuppa, A., Parello, F., Allard, P., Shinohara, H., Liuzzo, M., and Giudice, G.: New clues on the contribution of Earth's volcanism to the global mercury cycle, Bull Volcanol, 73, 497–510, https://doi.org/10.1007/s00445-010-0419-y, 2011.

Bagnato, E., Tamburello, G., Avard, G., Martinez-Cruz, M., Enrico, M., Fu, X., Sprovieri, M., and Sonke, J. E.: Mercury fluxes from volcanic and geothermal sources: an update, Geological Society, London, Special Publications, 410, 263–285, https://doi.org/10.1144/SP410.2, 2014.

Edwards, B. A., Pfeffer, M., Ilyinskaya, E., Aiuppa, A., Outridge, P., and Wang, F.: Mercury Emissions from the 2021 Fagradalsfjall Fissure Eruption, Iceland, AGU Fall meeting, 2021, V25B-0100, 2021.

Ferrara, R., Mazzolai, B., Lanzillotta, E., Nucaro, E., and Pirrone, N.: Volcanoes as emission sources of atmospheric mercury in the Mediterranean basin, Science of The Total Environment, 259, 115–121, https://doi.org/10.1016/S0048-9697(00)00558-1, 2000.

Friedli, H. R., Radke, L. F., Prescott, R., Pan, L., Woo, J.-H., and Carmichael, G. R.: Mercury in the atmosphere around Japan, Korea, and China as observed during the 2001 ACE-Asia field campaign: Measurements, distributions, sources, and implications, J. Geophys. Res., 109, D19S25, https://doi.org/10.1029/2003JD004244, 2004.

Mather, T. A., Witt, M. L. I., Pyle, D. M., Quayle, B. M., Aiuppa, A., Bagnato, E., Martin, R. S., Sims, K. W. W., Edmonds, M., Sutton, A. J., and Ilyinskaya, E.: Halogens and trace metal emissions from the ongoing 2008 summit eruption of Kīlauea volcano, Hawai`i, Geochimica et Cosmochimica Acta, 83, 292–323, https://doi.org/10.1016/j.gca.2011.11.029, 2012.

Schiavo, B., Morton-Bermea, O., Salgado-Martinez, E., Arellano, J., and Hernández-Álvarez, E.: Estimates of mercury flux and temporal variability of Hg/SO2 ratio in the plume of Popocatépetl volcano (Mexico), Journal of South American Earth Sciences, 101, 102614, https://doi.org/10.1016/j.jsames.2020.102614, 2020.

Shah, V., Jacob, D. J., Thackray, C. P., Wang, X., Sunderland, E. M., Dibble, T. S., Saiz-Lopez, A., Černušák, I., Kellö, V., Castro, P. J., Wu, R., and Wang, C.: Improved Mechanistic Model of the Atmospheric Redox Chemistry of Mercury, Environ. Sci. Technol., acs.est.1c03160, https://doi.org/10.1021/acs.est.1c03160, 2021.

Wardell, L. J., Kyle, P. R., and Counce, D.: Volcanic emissions of metals and halogens from White Island (New Zealand) and Erebus volcano (Antarctica) determined with chemical traps, Journal of Volcanology and Geothermal Research, 177, 734–742, https://doi.org/10.1016/j.jvolgeores.2007.07.007, 2008.